Journal of Solid State Chemistry **156,** 242–246 (2001)
doi:10.1006/jssc.2000.8996, available online at http://www.idealibrary.com on IDEAL®

Synthesis and Characterization of A New Open-Framework Cobalt Phosphate: $Cs_2Co_3(HPO_4)(PO_4)_2 \cdot H_2O$

Ray-Kuang Chiang,[1] Chi-Chun Huang, and Chun-Rong Lin

Department of Chemical Engineering, Far East College, Tainan, Taiwan 744, Republic of China

and

Ching-Shuei Wur

Department of Physics, National Cheng Kung University, Tainan, Taiwan 700, Republic of China

Received June 6, 2000; in revised form September 8, 2000; accepted October 6, 2000; published online January 3, 2001

A new cobalt phosphate $Cs_2Co_3(HPO_4)(PO_4)_2 \cdot H_2O$ 1, has been synthesized by hydrothermal reactions and characterized by single-crystal X-ray diffraction, thermogravimetric analysis, and magnetic techniques. It crystallizes in the monoclinic space group $P2_1$ with $a = 10.4711$ (6) Å, $b = 5.1129$ (3) Å, $c = 13.5584$ (8) Å, $\beta = 109.893$ (1)°, $V = 682.57$ Å^3, $Z = 2$. Refinement gave $R_1 = 0.0226$, w$R_2 = 0.0583$ for 2611 unique observed reflections ($I > 2\sigma(I)$). The cobalt and phosphorus atoms in 1 are tetrahedrally coordinated by oxygen atoms with Co to P ratio of 1. The framework structure of 1 is built up by sharing corners of $[Co(PO_4)]_2$ layers and $[Co(HPO_4)]$ double zigzag chains, which contains infinite 1-D tunnels, with 16-membered ring channels housing caesium cations and water molecules. Magnetic susceptibility measurements showed that 1 has a canted antiferromagnetic interaction at a transition temperature of about 10 K.

Key Words: **structure; caesium; cobalt phosphate.**

INTRODUCTION

Microporous framework structures containing a high level of transition metal centers are currently of great interest because of their potential catalytic applications. For example, much work has been done on the incorporation of divalent cobalt cations into aluminum (or gallium) phosphates (1–3). Several novel microporous cobalt phosphates with the formula of $MCoPO_4$ (M = Na, K, Rb, Cs, and NH_4^+) which are related to the zeolite ABW structure constructed by alternating CoO_4 and PO_4 tetrahedra have also been reported (4, 5). Using bifunctional amines as structure-directing agents in the hydrothermal (or solvothermal) syntheses has successfully led to many organically templated transition metal phosphates (6–15). Among them cobalt is of particular interest owing to its feasibility for tetrahedral coordination and potential catalytic properties. Organically templated cobalt phosphates showed a rich structure diversity varying from 1-D to 3-D (16–20). Classification of these compounds by unique structure building units is of substantial importance to the exploration of the possibility of cobalt phosphate adopting zeolitic structures. In the case of zinc phosphates, they have revealed several different structure features not found in zeolitic structures. These include the three (or four)-coordinated oxygen atoms, Zn–O–Zn linkages, and more flexible zinc oxygen coordination. Also, for divalent metal phosphates the charge density matching of framework host and template guest is not as easy as in zeolite structures. In aluminosilicates this can be done via replacing a fine-tuned amount of Si by Al, but in most of porous divalent metal phosphates a strictly alternating connection of M(II)O_4 and PO_4 is observed. Consequently, interrupted framework structures are frequently found in divalent metal phosphates with large pores, in which some oxygen atoms bond to only one tetrahedral atom. The interrupted structures are of interest, because some of them are related to the known zeolitic structure. Herein are described the synthesis and characterization of a new open-framework cobalt phosphate, $Cs_2Co_3(HPO_4)(PO_4)_2 \cdot H_2O$, with 16-ring channels. Its structure contains infinite Co–O–Co linkages and interrupted P–OH groups, and the major structural building unit, a double zigzag chain, is also a building unit in the known $CsCoPO_4$–ABW (5) structure.

EXPERIMENTAL

Synthesis

The syntheses were carried out in Teflon-lined acid digestion bombs with an internal volume of 23 cm^3 under

[1] To whom correspondence should be addressed. FAX: 886-6-598-7952. E-mail: raykuang@cc.fec.edu.tw.

0022-4596/01 $35.00

autogeneous pressure by heating the reaction mixture at 190°C for 3 days followed by slow cooling to room temperature at 4.8°Ch^{-1}. Compound **1** was prepared from the reaction mixture of $Co_3(PO_4)_2 \cdot xH_2O$ (1 mmole), 85% H_3PO_4 (4 mmole), piperazine (6 mmole), $H_2C_2O_4 \cdot 2H_2O$ (3 mmole), 50% CsOH water solution (6 mmole), distilled water (2.0 mL), and ethylene glycol (8.0 mL). The product was recovered by vacuum filtration and washed with copious distilled water. The product was a dark-blue needle-like crystal and a very small amount of dark-blue granular crystals. The XRD pattern of the blue needle compared well with the pattern simulated from the coordinates of the single-crystal study of **1** (see below). Preliminary analysis of the blue granular crystal showed that it is probably one form of $CsCoPO_4$, but the structure could not be solved because of the poor crystal quality.

Single-Crystal X-Ray Structure Analysis

The structure of **1** was determined by single-crystal X-ray methods, and the crystallographic data is summarized in Table 1. A suitable crystal ($0.80 \times 0.09 \times 0.09$ mm) was glued on a glass fiber and mounted on a smart CCD diffractometer using Mo$K\alpha$ radiation. Intensity data were collected for indexing in 1271 frames with increasing ω (width of 0.3° per frame). Unit cell dimensions for **1** were determined by a least-squares fit of 3291 reflections. Of the 4166 reflections collected, 2611 unique reflections were considered observed ($I_{obs} > 2\sigma(I)$). The absorption correction was based on symmetry-equivalent reflections using the *SADABS* programs (21). On the basis of systematic absences and statistic intensity distribution, the space group was determined to be $P\,2_1$. Direct methods were used to locate the Cs, Co, and P atoms first, and the remaining oxygen atoms were found from successive difference maps. O(13) was assigned as water. Bond valence calculations (22) indicated that O(6) and O(10) have values of 1.56 and 1.17, respectively, and all other oxygen atoms have values ranging from 1.87 to 2.00. O(6) and O(10) were thus assigned as pendant oxygen atom and OH, respectively. The three H atoms were then located on difference Fourier maps. The final cycles of refinement, including the atomic coordinates and anisotropic thermal parameters for all nonhydrogen atoms and fixed atomic coordinates and isotropic thermal parameters for the hydrogen atoms, converged at $R_1 = 0.0227$ and w$R_2 = 0.0578$. In the final difference map the deepest hole was -0.72 e Å^{-3} and the highest peak 0.69 e Å^{-3}. Anomalous and secondary extinction corrections were applied. All calculations were performed using the *SHELXTL* programs (23). Supplementary data (X-ray crystallographic file in CIF format, and observed and calculated structure factors) are available from the authors.

Thermogravimetric analysis was carried out in nitrogen at a heating rate of 10°C/min (Perkin–Elmer Instruments, TGA 7). Magnetic susceptibility was measured under 5000 Oe from 2 to 300 K (SQUID, Quantum Design).

TABLE 1
Crystallographic Data

	$Cs_2Co_3(HPO_4)(PO_4)_2 \cdot H_2O$
*F*w	746.54
Crystal system	monoclinic
Size (mm)	$0.80 \times 0.09 \times 0.09$
Habit	blue needle
Space group	$P2_1$
a (Å)	10.4711(6)
b (Å)	5.1129(3)
c (Å)	13.5584(8)
β (deg)	109.893(1)
V (Å^3)	682.57(7)
Z	2
Temp (K)	293(2)
λ, (Å)	0.71073
*T*max/min	0.9508 and 0.7981
ρ_{calcd} (gcm^{-3})	3.632
μ, cm^{-1}	92.72
F(000)	686
$2\theta_{max}$	56.50
Observed reflections [$I > 2s(I)$]	2611
Parameter refined	190
Final *R* indices [$I > 2$sigma(I)]	$R1^a = 0.0227$, w$R_2^b = 0.0578$
R indices (all data)	$R1 = 0.0246$, w$R_2 = 0.0589$

[a] $R_1 = \sum||F_o| - |F_c||/\sum|F_o|$.

[b] w$R_2 = [\sum w(|F_o|^2 - |F_c|^2)^2/\sum w(|F_o|^2)^2]^{1/2}$, $w = [\sigma^2(F_o^2) + 0.0288\,P]^2 + 1.2501P]$, where $P = (F_o^2 + 2F_c^2)/3$.

RESULTS AND DISCUSSION

Crystal Structure of $Cs_2Co_3(HPO_4)(PO_4)_2 \cdot H_2O$

The atomic coordinates and the thermal parameters of **1** are given in Table 2, and selected bond lengths and bond valence sums are given in Table 3. The projection of the structure along [010] is shown in Fig. 1. The structure contains cross-shaped 16-ring windows built up by edges of alternating PO_4 and CoO_4 tetrahedra, which caesium cations and water molecules inhabit. The cobalt and phosphorus atoms in **1** are tetrahedrally coordinated by oxygen atoms with Co to P ratio of 1. The framework has hydrogen bonding with the occluded water molecules, O(10) $\cdots$ O(13) = 2.87 Å, and the water molecules in the center of the hole are hydrogen bonded to each other, O(13) $\cdots$ O(13) = 2.99 and 3.02 Å. While the short distance between O(6) and O(10) indicates hydrogen bonding might exist, the small angle of $\angle$ O(10)–H $\cdots$ O(6) is unacceptable for hydrogen bonding. The coordination numbers of the two unique caesium atoms are 7 and 11 respectively, and were determined on the basis of the maximum gap occurring in the Cs–O distances list. The maximum cation–oxygen distance for Cs–O, 3.60 Å, according to Donny and

TABLE 2
Atomic Coordinates and Thermal Parameters for 1

Atom	x	y	z	U_{eq}[a]
Cs(1)	0.4976(1)	0.2422(1)	0.2783(1)	0.034(1)
Cs(2)	0.0057(1)	0.2243(1)	0.2551(1)	0.024(1)
Co(1)	0.8357(1)	0.7490(2)	0.3973(1)	0.018(1)
Co(2)	0.1196(1)	0.2057(2)	0.0006(1)	0.016(1)
Co(3)	0.6095(1)	0.2812(2)	0.0086(1)	0.014(1)
P(1)	0.6974(1)	− 0.2434(3)	0.1455(1)	0.012(1)
P(2)	0.2039(1)	0.7531(3)	0.1304(1)	0.015(1)
P(3)	0.8395(1)	0.2511(3)	0.5274(1)	0.016(1)
O(1)	0.7077(4)	− 0.3169(9)	0.2556(3)	0.019(1)
O(2)	0.5682(4)	− 0.3850(7)	0.684(3)	0.015(1)
O(3)	0.8215(4)	− 0.3397(9)	0.1203(3)	0.025(1)
O(4)	0.6786(4)	0.0521(7)	0.1285(3)	0.021(1)
O(5)	0.0658(4)	0.8783(8)	0.0602(3)	0.022(1)
O(6)	0.2307(5)	0.8200(10)	0.2434(3)	0.032(1)
O(7)	0.3083(4)	0.8939(9)	0.0909(3)	0.025(1)
O(8)	0.2024(5)	0.4578(8)	0.1115(4)	0.032(1)
O(9)	0.0182(4)	0.6934(10)	0.3951(3)	0.024(1)
O(10)	0.7387(4)	0.1328(8)	0.5790(3)	0.025(1)
O(11)	0.8138(4)	0.5455(8)	0.5124(3)	0.022(1)
O(12)	0.8106(5)	0.1192(8)	0.4219(3)	0.025(1)
O(13)	0.4520(6)	0.2010(20)	0.5328(8)	0.113(4)
H(10)	0.6755	0.0468	0.5434	0.05
H(13A)	0.4906	0.2440	0.5888	0.05
H(13B)	0.4793	0.0473	0.5376	0.05

[a] U_{eq} is defined as one-third of the trace of the orthogonalized U_{ij} tensor.

TABLE 3
Selected Bond Lengths (Å) and Bond Valence Sums ($\sum$s) for 1

Cs(1)-O(7)	3.183(4)	Cs(1)-O(4)	3.360(4)
Cs(1)–O(1)	3.237(4)	Cs(1)–O(13)	3.379(9)
Cs(1)–O(12)	3.254(4)	Cs(1)–O(6)	3.434(5)
Cs(1)–O(8)	3.336(4)		
$\sum$s(Cs(1)–O) = 0.64			
Cs(2)–O(9)	3.034(4)	Cs(2)–O(5)	3.412(4)
Cs(2)–O(3)	3.104(4)	Cs(2)–O(8)	3.491(5)
Cs(2)–O(6)	3.178(5)	Cs(2)–O(10)	3.534(4)
Cs(2)–O(11)	3.208(4)	Cs(2)–O(12)	3.567(4)
Cs(2)–O(9)	3.289(5)	Cs(2)–O(3)	3.602(4)
Cs(2)–O(4)	3.384(4)		
$\sum$s(Cs(1)–O) = 0.99			
Co(1)–O(9)	1.942(4)	Co(1)–O(12)	1.942(4)
Co(1)–O(11)	1.954(4)	Co(1)–O(1)	1.954(4)
$\sum$s(Co(1)–O) = 1.98			
Co(2)–O(8)	1.946(4)	Co(2)–O(5)	2.020(4)
Co(2)–O(3)	1.952(4)	Co(2)–O(5)	2.034(4)
$\sum$s(Co(2)–O) = 1.81			
Co(3)–O(7)	1.919(4)	Co(3)–O(2)	1.988(4)
Co(3)–O(4)	1.933(4)	Co(3)–O(2)	1.999(4)
$\sum$s(Co(3)–O) = 1.95			
P(1)–O(1)	1.506(4)	P(1)–O(3)	1.534(4)
P(1)–O(4)	1.531(4)	P(1)–O(2)	1.576(4)
$\sum$s(P(1)–O) = 4.94			
P(2)–O(6)	1.501(5)	P(2)–O(7)	1.549(4)
P(2)–O(8)	1.530(5)	P(2)–O(5)	1.572(4)
$\sum$s(P(2)–O) = 4.98			
P(3)–O(12)	1.516(4)	P(3)–O(9)	1.532(4)
P(3)–O(11)	1.531(4)	P(3)–O(10)	1.572(4)
$\sum$s(P(3)–O) = 4.95			

Allmann was also considered (24). The bond valence sum of Cs(1) is much less than 1, indicating it is loosely bonded.

The framework of **1** can be considered as being built up by corner-sharing of two structure units, the $[Co(HPO_4)]$ chain and the $[CoPO_4]$ layer, Fig. 2. This results in much smaller 3-ring and 4-ring windows along the [001] direction, and 6-ring windows along the [100] direction (Fig. 3). In both structure units they contain the edge-sharing four-ring chain, the so-called double zigzag (dz) chain. The first dz chain contains a 2_1 screw axis in the center of the chain along the *b* axis involving P(3) and Co(1) tetrahedra. The second dz chain in the layer involves P(1), P(2), Co(2), and Co(3) tetrahedra, and the neighboring dz chains are fused by μ-3 oxygen atoms, O(2) and O(5), to form a layer of alternating three-ring and four-ring chains. This leads to the formation of the infinite –Co–O–Co– linkages, Co(2)–O(5)–Co(2) and Co(3)–O(2)–Co(3). The neighboring dz chains in the layer are also related by 2_1 symmetry operations that sit in the center of the three-ring chain. A similar layer has been found in zinc phosphate (15), but this is the first example in the cobalt phosphates. The Co–O bond lengths are in the range 1.919(4)–2.020(4) Å, and the longer ones are bonded to the μ-3 oxygen atoms. The P–O bond lengths are in the range 1.501(5)–1.576(4) Å, and the longest three are related to P–O(10)–H and the two bonded to μ-3 oxygen atoms, P–O(2) and P–O(5). The shortest is related to the pendant P–O(6).

Other cobalt phosphates containing layers with three-ring and four-ring chains are $[H_3N(CH_2)_3NH_3]_{0.5}$

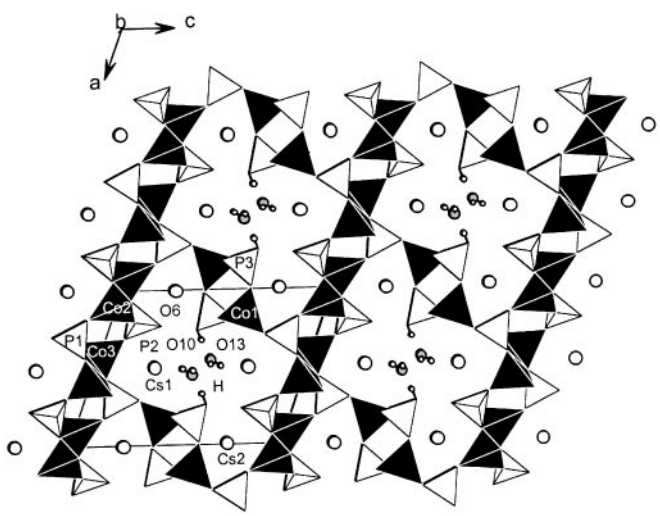

FIG. 1. Polyhedral view of **1** showing the 16-ring tunnels along the [010] direction.

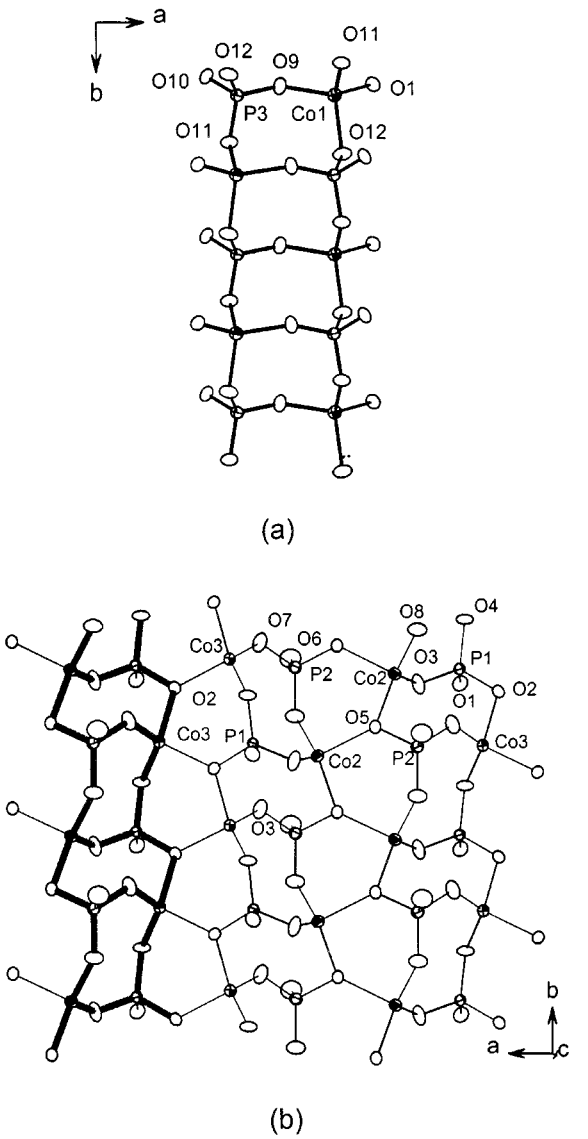

FIG. 2. Structure units of **1** showing the connection of Co and P atoms in the dz chains (a) and in the $[CoPO_4]$ layer (b).

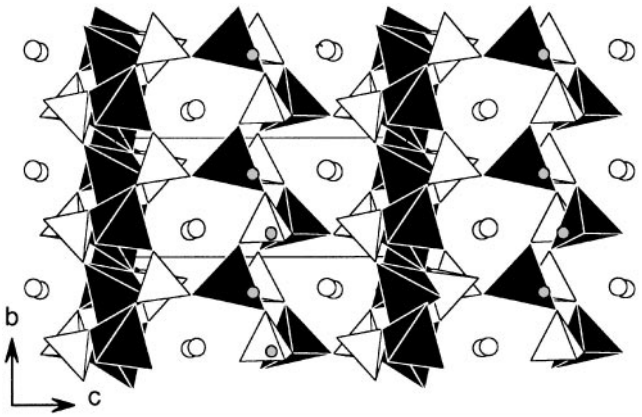

FIG. 3. Polyhedral view of **1** showing the 6-ring tunnels along the [100] direction: CoO_4, dark tetrahedral; PO_4, light tetrahedral; caesium, large circle; water, small circle.

$CoPO_4 \cdot 0.5H_2O$ and $[H_3N(CH_2)_4NH_3]_{0.5}CoPO_4$, in which the building unit, the corner-sharing four-ring chains, is different from what is found in **1**. The documented caesium cobalt phosphate structures are rare. $Cs_2Co(PO_4)_3$ (25) and $CsCoPO_4$–ABW (5) are the only two examples. $Cs_2Co(PO_4)_3$ contains infinite PO_3 chains linked by CoO_6 octahedra, which is not related to compound **1**. Interestingly, compound **1** and $CsCoPO_4$ both utilize the dz chains as their structural building unit. In $CsCoPO_4$ the dz chains are connected with strictly alternating CoO_4 and PO_4 tetrahedra, while in compound **1** the dz chains are connected in a way involving three-coordinated oxygen atoms and interrupted P–OH. The difference indicates that compound **1** can utilize more flexible connections to adapt the host–guest charge matching. From this evidence and some structure features found in zinc phosphates, the possibility of cobalt phosphates adopting the known zeolite-like structure type is probably limited, but the cobalt phosphates with ample structure diversity like zinc phosphates are predictable. Another related compound is $CsZn_3(HPO_4)_2(PO_4)$. It contains an interrupted open framework with more slender 16-ring channels which only Cs cations inhabit, and the building units in it are the dz chain and a single zigzag chain (26).

Thermogravimetric decomposition of compound **1** was carried out in N_2 from 30 to 1000°C and showed unresolved two steps. The first step ranging from 50 to $\sim$370°C is attributed to the evaporation of occluded water. The second step ranging from $\sim$370 to 650°C is attributed to the removal of water that is formed by the condensation of HO–P groups. The total weight lost (4.2%) is a little higher than the theoretical value (3.6%). The XRD of the residual of the TGA experiment showed peaks of the unidentified blue granular crystals found in the hydrothermal reaction. They are probably one form of $CsCoPO_4$. Further work on the blue granular crystals is needed to prove this.

The variable temperature magnetic susceptibility for **1** is shown in Fig. 4. The linear behavior of $1/\chi(T)$ above 25 K obeys well the Curie–Weiss equation ($C = 7.4$ emu-K/mol, $\theta = -27.4$ K). The effective magnetic moment per metal atom at 300 K, 4.26 μ_B, is greater than the spin-only value (3.87 μ_B), indicating the existence of a significant orbital contribution, which is commonly found in cobalt compounds. The negative Weiss temperature is characteristic of an antiferromagnetic interaction, but below 25 K the magnetic susceptibility rises abruptly with a maximum at 6 K indicating some ferromagnetic contribution. Also, the χT at about 10 K rises sharply to a maximum at $\sim$7 K and then decreases as sharply. This weak ferromagmetic contribution

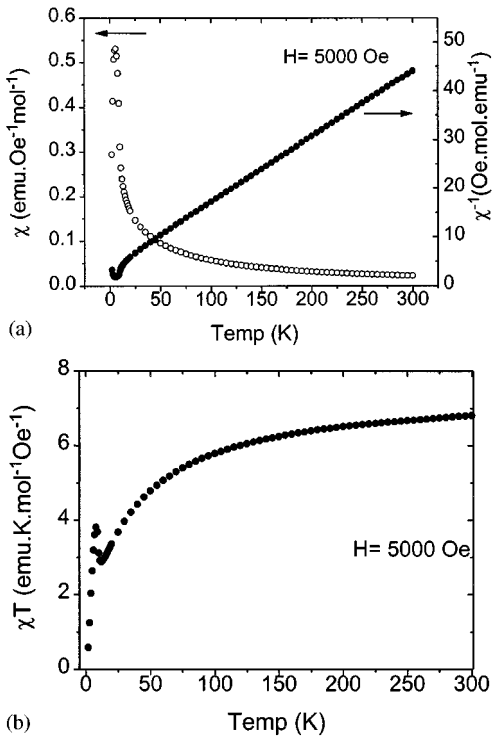

FIG. 4. Temperature-dependent magnetic susceptibility data for **1**: χ vs T and χ^{-1} vs T, and χT vs T.

could be due to unequal antiferromagnetic spin compensation of two nonequivalent Co(II) ions. This might result from the interaction of the nearest neighbor Co^{2+} in the infinite –Co–O–Co– chains. At even lower temperature the ferromagnetic contribution disappears and three-dimensional antiferromagnetic interaction occurs. This probably arises from the interchain interaction via the Co–O–P–O–Co pathway.

ACKNOWLEDGMENTS

R.K.C. thanks Far East College and the National Science Council of the Republic of China (NSC 88-2113-M-269-001) for support, and Professor S. L. Wang and Ms. F.-L. Liao at National Tsing Hua University for X-ray intensity data collection.

REFERENCES

1. P. Feng, X. Bu, and G. D. Stucky, *Nature* **388,** 735 (1997).
2. X. Bu, P. Feng, and G. D. Stucky, *Science* **278,** 2080 (1997).
3. X. Bu, T. E. Gier, P. Feng, and G. D. Stucky, *Chem. Mater.* **10,** 2546 (1998).
4. P. Feng, X. Bu, S. Tolber, and G. D. Stucky, *J. Am. Chem. Soc.* **119,** 2497 (1997).
5. P. F. Henry, E. M. Hughes, and M. T. Weller, *J. Chem. Soc. Dalton Trans.*, 555 (2000).
6. R. C. Haushalter and L. A. Mundi, *Chem. Mater.* **4,** 31 (1992).
7. M. I. Khan, L. M. Meyer, R. C. Hausshalter, A. L. Schweitzer, J. Zubieta, and J. L. Dye, *Chem. Mater.* **8**(1), 43 (1996).
8. K.-H. Lii, Y.-H. Huang, V. Zima, C.-Y. Huang, H.-M. Lin, Y. C. Jiang, F.-L. Liao, and S.-L. Wang, *Chem. Mater.* **10,** 2599 (1998).
9. A. Choudhury, S. Natarajan, and C. N. R. Rao, *Chem. Commun.* 1305 (1999).
10. W. T. A. Harrison and L. Hannooman, *J. Solid State Chem.* **131,** 363 (1997).
11. S. Neeraj, S. Natarajan, and C. N. R. Rao, *Chem. Commun.*, 165 (1999).
12. D. Chidambaram and S. Natarajan, *Mater. Res. Bull.* **33**(8), 1275 (1998).
13. G.-Y. Yang and S. C. Sevov, *J. Am. Chem. Soc.* **121,** 8389 (1999).
14. J. Chen, R. Jones, S. Natarajan, M. B. Hursthouse, and J. M. Thomas, *Angew. Chem. Int. Ed. Engl.* **33**(6), 639 (1994).
15. S. Ekambaram and S. C. Sevov, *Angew. Chem. Int. Ed.* **38**(3), 372 (1999).
16. J. R. D. DeBord, R. C. Haushalter, and J. Zubieta, *J. Solid State Chem.* **125,** 270 (1996).
17. A. R. Cowley and A. M. Chippindale, *J. Chem. Soc. Dalton Trans.*, 2147 (1999).
18. C. N. R. Rao, S. Natarajan, and S. Neeraj, *J. Am. Chem. Soc.* **122,** 2810 (2000).
19. S. Natarajan, S. Neeraj, A. Choudhury, and C. N. R. Rao, *Inorg. Chem.* **39,** 1426 (2000).
20. H.-M. Yuan, J.-S. Chen, G.-S. Zhu, J.-Y. Li, J.-H. Yu, G.-D. Yang, and R.-R. Xu, *Inorg. Chem.* **39,** 1476 (2000).
21. G. M. Sheldrick, *SADABS*, Siemens Analytical X-Ray Instrument Division, Madison, WI, 1995.
22. I. D. Brown and D. Altermatt, *Acta Crystallogr. B* **41,** 244 (1985).
23. G. M. Sheldrick, *SHELXTL Programs*, Version 5.1, Brucker AXS, 1998.
24. G. Donny and R. Allmann, *Am. Mineral.* **55,** 1003 (1970).
25. V. A. Efremov, V. V. Ilyukhin, A. V. Lavrov, and A. M. Turchaninov, *Dokl. Akad. Nauk SSSR* **278,** 103 (1984).
26. P. Feng, X. Bu, and G. D. Stucky, *Acta Crystallogr. C* **53,** 1170 (1997).